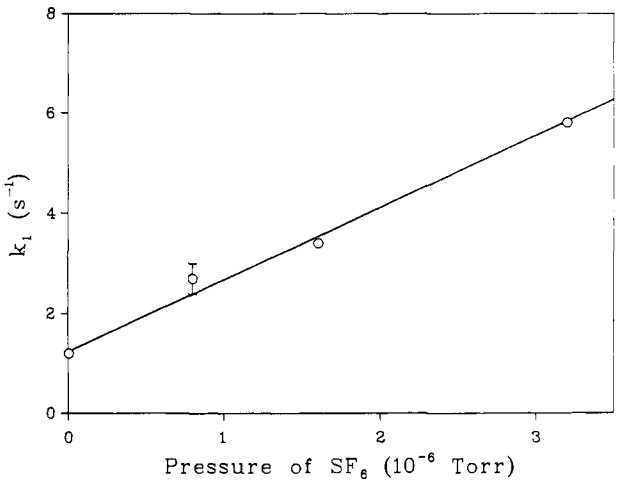

Figure 5. Collisional cooling rate constants k_1 as a function of SF_6 pressure. Each point is derived from the slope of a plot like that of Figure 4.

the derivative of the first-order cooling rate constant with respect to pressure (units of cm^3 $molecule^{-1}$ s^{-1}. Then the overall relaxation rate constant k_1 is expressed as

$$k_1 = k_r + k_p P \quad (4)$$

where k_r is the radiative cooling rate constant, and P is the pressure of neutrals.

The resulting bimolecular rate constants for cooling of hot ions were 9×10^{-12} cm^3 $molecule^{-1}$ s^{-1} for Ar and 4.5×10^{-11} cm^3 $molecule^{-1}$ s^{-1} for SF_6. For Ar, the cooling rate constant is 0.016 times the calculated orbiting rate constant, while for SF_6 the ratio is 0.06. Thus it requires 50 collisions for Ar to remove half the excess internal energy, while this requires 12 collisions for SF_6.

For both of these neutrals, the collisional efficiency of cooling is low, but it is in line with observations of cooling of other similar-sized ions by these same two neutrals. It was found that it requires 77 argon collisions to cool bromobenzene ion from 2.5 to 0.25 eV excess energy,[15] which corresponds to a bimolecular cooling rate constant of 1.6×10^{-11} cm^3 $molecule^{-1}$ s^{-1}; and it requires 5 collisions for SF_6 to cool benzene ion from 2.8 to 1.5 eV, a bimolecular cooling rate constant of 8×10^{-11} cm^3 $molecule^{-1}$ s^{-1}.[16] The present results are thus quite comparable to the situation found for bromobenzene and benzene ion quenching.

(15) Ahmed, M. S.; Dunbar, R. C. *J. Am. Chem. Soc.* **1987**, *109*, 3215.
(16) Ahmed, M. S.; Dunbar, R. C. *J. Chem. Phys.* **1988**, *89*, 4829.

Conclusions

The competitive-dissociation ion thermometry technique described here provides a convenient way of probing the internal energy of the ions at a chosen moment in time and in a region of space defined by the laser beam. Various diagnostic applications can be imagined in the study of physical and chemical processes involving heating or cooling of ions. Examples might be the study of energy deposition in charge-transfer ionization or multiphoton ionization of dioxane, or the study of collisional heating of dioxane ions by energetic ion-neutral collisions.

The ion for which competitive dissociation has been most thoroughly calibrated as a function of internal energy is *n*-butylbenzene ion, and this system is often considered as a standard test case for assessing ion excitation in mass spectrometers.[11] The competition to form $C_7H_7^+$ and $C_7H_8^+$ product ions has been measured as a function of parent ion internal energy for ions of well-characterized energy by charge-transfer ionization, by ICR photodissociation, and by photoelectron–photoion coincidence. For photodissociation work in the visible wavelength region dioxane ion is more convenient, because the m/z 57/58 ratio which serves the thermometric function is near unity, whereas for *n*-butylbenzene the m/z 91/92 ratio is closer to 0.1. The calibration for dioxane ion given here in Figure 2 is believed to be as precise and reliable as that for *n*-butylbenzene ion.

The collisionless cooling of dioxane ion in this energy regime, with a time constant of 1.0 s, is one of the slowest processes involving isolated ions which has been observed in the laboratory. Consideration of the slow radiative equilibration of an isolated ion with the environment is relevant to understanding deep-space chemistry of polyatomic molecules, and is increasingly important in mass spectrometry as the use of ion-trapping instruments increases.

The collisional cooling of dioxane ion by Ar and SF_6 affords no surprises, proceeding with collisional efficiencies typical for such systems. In the case of SF_6, collisional cooling is much slower than predicted by a full-equilibration model (in which the internal energy is statistically equilibrated between ion and neutral on each collision). Again, this is similar to what is observed in other comparable systems.[15] For argon quenching, the full-equilibration model is harder to specify, but the very inefficient quenching observed here is certainly slower than a full-equilibration prediction based on statistical partitioning into the argon translational degrees of freedom.

Acknowledgment. Appreciation is expressed to the National Science Foundation and to the donors of the Petroleum Research Fund, administered by the American Chemical Society, for support of this research.

Optical Properties of Metalloporphyrin Excited States

Juan Rodriguez, Christine Kirmaier, and Dewey Holten*

Contribution from the Department of Chemistry, Washington University, St. Louis, Missouri 63130. *Received February 7, 1989*

Abstract: The absorption features of $^1(\pi,\pi^*)$, $^3(\pi,\pi^*)$, $^3(d,\pi^*)$, and (d,d) excited states of metalloporphyrins have been closely examined between 420 and 900 nm with subpicosecond/picosecond transient absorption spectroscopy. The spectra of all of these excited states exhibit strong but not readily distinguishable absorption between the Soret- and Q-band bleachings, a region used extensively and often exclusively in transient absorption studies on porphyrins. The absorption features between 600 and 900 nm are smaller than those observed in the Soret region but have distinctive characteristics that aid in assessing the presence or absence of a particular type of transient state. We discuss the electronic origins of the prominent bands in the excited-state spectra. Our results and discussion provide fundamental information on the optical properties of metalloporphyrin excited states and a much needed framework for better interpreting the results of in vivo and in vitro transient absorption studies on these complexes.

Transient absorption spectroscopy has played a central role in furthering the understanding of the primary charge-separation process in bacterial photosynthetic reaction centers,[1] the photoinduced release/rebinding of diatomic ligands from hemoglobin

0002-7863/89/1511-6500$01.50/0

Table I. Summary of Metalloporphyrin (π,π^*) Excited-State Absorption Spectra[a]

	ground-state Q(1,0) absn		$^1(\pi,\pi^*)$				$^3(\pi,\pi^*)$			
			blue absn		stim emiss[b]		blue absn		red absn	
compd	λ_{max}	ϵ	λ_{max}	$\Delta\epsilon$	λ_{max}	$\Delta\epsilon$	λ_{max}	$\Delta\epsilon$	λ_{max}	$\Delta\epsilon$
$Sn^{IV}OEPCl_2$	538	15	455	38	644	4	440	35	713	3
$Sn^{IV}TPPCl_2$	560	18	457	45	660	6	490	44	820	5
$Zn^{II}OEP$	534	18	450	55	638	6	437	55	755	7
$Zn^{II}TPP$	552	20	450	71	655	9	460	87	832	9
$Mg^{II}OEP$	542	18	455	46	638	10	442	39	790	8
$Mg^{II}TPP$	565	20	456	65	665	7	455	58	840	6
H_2OEP	500	18	432	42	693	5	438	42	*c*	3
H_2TPP	513	20	440	51	725	4	442	77	784	7
$Cu^{II}OEP$	527	13					433	47	750	7
$Cu^{II}TPP$	542	13					470	31	840	4

[a] Spectra measured in CH_2Cl_2 except for the Mg(II) and free-base complexes, which were studied in toluene/20% MeI. The wavelength maxima (λ_{max}) are given in nanometers, and the differential coefficients ($\Delta\epsilon$) are given in mM^{-1} cm^{-1}. The ground-state Q(1,0) extinction coefficients (mM^{-1} cm^{-1}) were taken from ref 4, 9a, and 17b-d. [b] Q(0,1) stimulated emission band. [c] No clear peak in the broad transient absorption is resolved.

and myoglobin,[2] and the photophysics and photochemistry of metalloporphyrins and related molecules.[3] Ultrafast transient absorption measurements on these complexes hold much promise not only for elucidating the photodynamics of metalloporphyrins in vivo and in vitro but also for advancing our knowledge of such fundamental processes as electronic and vibrational relaxation, solvent dynamics, photodissociation, and energy and electron transfer, to name a few.

A present limitation of transient absorption spectroscopy of metalloporphyrins is that too often one is faced with the task of assigning a spectrum without a clear understanding of which features are characteristic of a particular excited state. For example, although a number of $^1(\pi,\pi^*)$ and $^3(\pi,\pi^*)$ spectra have been reported (see ref 3–6 and citations therein), the results are generally fragmentary and have not established which spectral features, if any, best characterize these states, and why. Similarly, it has also not been determined how to spectrally distinguish (π,π^*) states of the porphyrin ring, metal ↔ ring (d,π^*) and (π,d) charge-transfer states, and metal (d,d) states. The lack of a broad understanding of metalloporphyrin excited-state spectra hinders assignment of absorption changes observed in systems where one or more of these excited states may serve as an electron donor or acceptor or as a precursor for the transient binding or release of axial ligands. It is essential, to properly interpret ultrafast time scale measurements, to understand which features in a transient absorption spectrum are unique to a particular type of state and thus can be used with a high degree of certainty as spectroscopic signatures. The purpose of this paper is to add such fundamental new information on the optical spectroscopy of metalloporphyrin excited states.

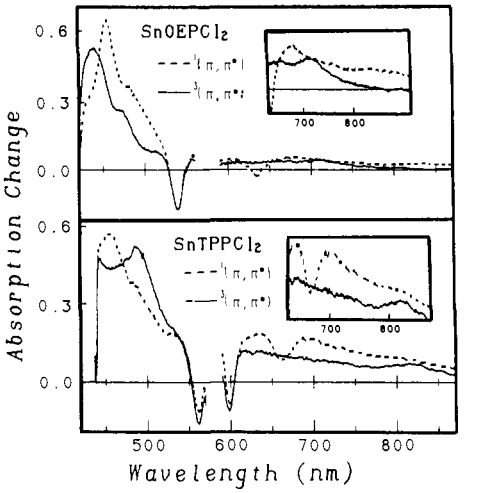

Figure 1. Absorption difference spectra for the $^1(\pi,\pi^*)$ (---) and $^3(\pi,\pi^*)$ (—) excited states of $Sn^{IV}OEPCl_2$ (top panel) and $Sn^{IV}TPPCl_2$ (lower panel) in CH_2Cl_2. The singlet and triplet spectra were acquired 20 ps and 3 ns, respectively, after a 350-fs flash at 582 nm. The insets show the near-infrared region on an expanded scale.

Experimental Section

Most of the metalloporphyrins used in these studies were obtained from Porphyrin Products, except for ZnOEP and ZnTPP, which were supplied by Aldrich. The purity of the samples was checked by UV/vis absorption and fluorescence spectra; samples were chromatographed on basic alumina where necessary. Static or flowed samples generally having a concentration of about 100 μM in spectral grade solvents were investigated in 2-mm path length optical cells. Time-resolved absorption difference spectra were obtained by using either a spectrometer employing 30-ps, ~500-μJ excitation flashes at 532 nm[7a] or an apparatus employing 350-fs, ~200-μJ excitation flashes at 582 nm[7b] that were focused to a spot size of 1.5–2 mm at the sample. Under these conditions the fraction of molecules placed in the excited state ranged from 10% to 30%.[7c] Both instruments employ dual-beam detection using a white-light

(1) Kirmaier, C.; Holten, D. *Photosynth. Res.* **1988**, *13*, 225–260.
(2) Hochstrasser, R. M.; Johnson, C. K. In *Ultrashort Laser Pulses*; Kaiser, W., Ed.; Springer-Verlag: New York, 1988; p 357.
(3) (a) Holten, D.; Gouterman, M. In *Optical Properties and Structure of Tetrapyrroles*; Blauer, G., Ed.; de Gruyter: Berlin, 1985; p 63. (b) Dzhagarov, B. M.; Chirvonyi, V. S.; Gurinovich, G. P.; In *Laser Picosecond Spectroscopy and Photochemistry of Biomolecules*; Letokov, V. S., Ed.; Hilger: Bristol, 1987; p 137.
(4) Pekkarinen, L.; Linschitz, H. *J. Am. Chem. Soc.* **1960**, *82*, 2407–2411.
(5) (a) Magde, D.; Windsor, M. W.; Holten, D.; Gouterman, M. *Chem. Phys. Lett.* **1974**, *29*, 183–188. (b) Harriman, A. *J. Chem. Soc., Faraday Trans. 2* **1981**, *77*, 1281–1291. (c) Cornelius, P. A.; Steele, A. W.; Chernoff, D. A.; Hochstrasser, R. M. *Chem. Phys. Lett.* **1981**, *82*, 9–14. (d) Kalaya-nasundaram, K.; Neumann-Spallart, M. *J. Phys. Chem.* **1982**, *86*, 5163–5169. (e) Serpone, N.; Netzel, T. L.; Gouterman, M. *J. Am. Chem. Soc.* **1982**, *104*, 246–252. (f) Ponterini, G.; Serpone, N.; Bergkamp, M. A.; Netzel, T. L. *J. Am. Chem. Soc.* **1983**, *105*, 4639–4645; (g) Reynolds, A. H.; Straub, K. D.; Rentzepis, P. M. *Biophys. J.* **1982**, *40*, 27–31. (h) Rillema, D. P.; Nagle, J. K.; Barringer, L. F., Jr.; Meyer, T. J. *J. Am. Chem. Soc.* **1984**, *106*, 3937–3943. (i) Kim, D.-H.; Holten, D.; Gouterman, M. *J. Am. Chem. Soc.* **1984**, *106*, 2793–2798. (j) Irvine, M. P.; Harrison, R. J.; Strahand, M. A.; Beddard, G. S. *Ber. Bunsenges Phys. Chem.* **1985**, *89*, 226–232. (k) Kalay-anasundaram, K.; Shelnutt, J. A.; Gratzel, M. *Inorg. Chem.* **1988**, *27*, 2820–2825. (l) Kikuchi, K.; Kurabayashi, Y.; Kokubun, H.; Kaizu, Y.; Kobayashi, H. *J. Photochem. Photobiol. A* **1988**, *45*, 261–263.
(6) (a) Tait, C. D.; Holten, D.; Barley, M. H.; Dolphin, D.; James, B. R. *J. Am. Chem. Soc.* **1985**, *107*, 1930–1934. (b) Levine, L. M. A.; Holten, D. *J. Phys. Chem.* **1988**, *92*, 714–720. (c) The near-infrared difference spectra of the $^3(d,\pi^*)$ states of $Ru^{II}TPP(pip)_2$ and $Ru^{II}TPP(py)_2$ are the same at 295 and 77 K.[6d] This shows that the $^3(d,\pi^*)$ spectra of Figure 5 (dashed) and Figure 6 do not contain a thermal contribution from the spectra of the $^3(\pi,\pi^*)$ states; (d) Rodriguez, J.; McDowell, L.; Holten, D. *Chem. Phys. Lett.* **1988**, *147*, 235–240.
(7) (a) Kim, D.-H.; Kirmaier, C.; Holten, D. *Chem. Phys.* **1983**, *75*, 305–322. (b) Kirmaier, C.; Holten, D.; Bylina, E. J.; Youvan, D. C. *Proc. Natl. Acad. Sci. U.S.A.* **1988**, *85*, 7562–7566. (c) By our estimates, less than 10% of the molecules that had been excited subsequently absorb a second photon. In one of the samples (NiTPP) we experimented with tighter focusing of the excitation pulse to obtain an estimate of the contribution of direct two-photon absorption. At photon intensities about 3 times greater than those normally used (10^{11} W/cm^2) we were able to observe a deviation from linearity that corresponded to an additional 2–3% of the ground-state molecules being excited by this nonlinear process. This yields a cross-section estimate for two-photon absorption at 582 nm in the range 10^{-49}–10^{-48} cm^4 photon^{-1} molecule^{-1} s, which agrees with the expected value for metalloporphyrins.[28b] Thus, under normal excitation conditions, two-photon processes are generally insignificant.

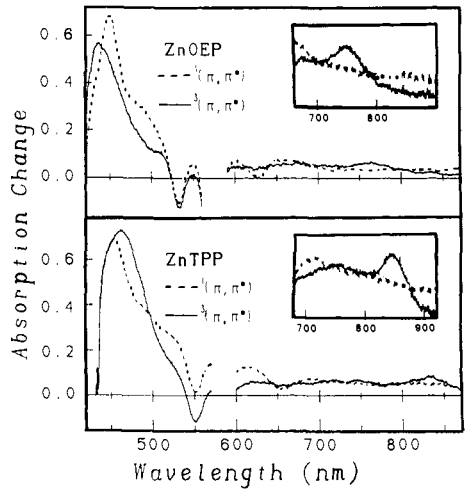

Figure 2. Absorption difference spectra for the $^1(\pi,\pi^*)$ (---) and $^3(\pi,\pi^*)$ (—) excited states of $Zn^{II}OEP$ (top panel) and $Zn^{II}TPP$ (lower panel) in CH_2Cl_2. The singlet and triplet spectra were measured 20 ps and 3 ns, respectively, after excitation with a 350-fs flash at 582 nm. The insets show spectra in the near-infrared region on an expanded scale, obtained 30 ps (---) and 12 ns (—) after excitation with a 30-ps 532-nm flash.

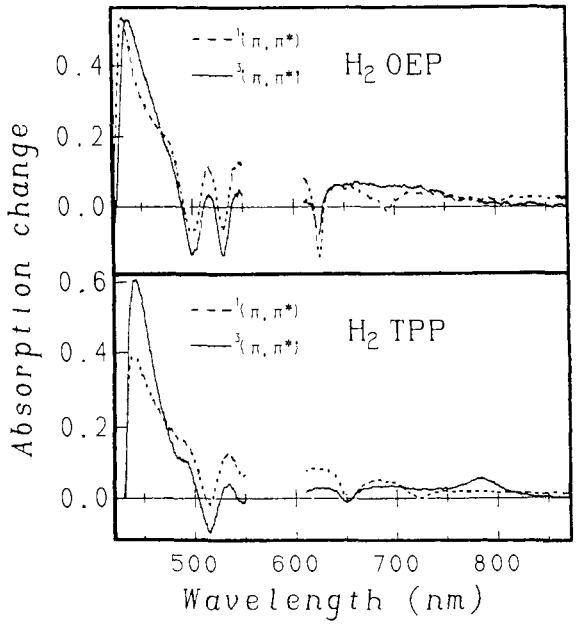

Figure 3. Absorption difference spectra for the $^1(\pi,\pi^*)$ (---) and $^3(\pi,\pi^*)$ (—) excited states of H_2OEP (top panel) and H_2TPP (lower panel) in toluene:MeI = 4:1. The singlet and triplet spectra were measured 3 ps and 3.6 ns after excitation with a 350-fs 582-nm flash.

probe pulse and a vidicon-based data-acquisition system with a 150-nm spectral window movable throughout the visible and near-infrared. A typical transient absorption spectrum encompassing a 150-nm wavelength interval is obtained by averaging the data from about 300 pulses and has a resolution in ΔA of ±0.005. Complete spectra covering a larger wavelength region (normally 420–900 nm) were constructed from the data acquired in overlapping 150-nm intervals.

Transient absorption difference spectra from 420 to past 900 nm were acquired for a large series of porphyrins. For each complex complete spectra were measured with a fixed experimental setup (i.e., the same sample and excitation conditions), so that the absorption changes across the entire spectral region could be compared directly without having to make assumptions concerning scaling factors associated with extent of excitation, etc. Thus, the absorption changes in the Soret region are necessarily large (i.e., ΔA = 0.4–0.6) so that absorption changes in the near-infrared (0.05–0.15) would be significantly above experimental error (±0.005). These absorption changes are well within the dynamic range of the spectrometers. The position and shape of the features in the near-infrared were checked by reproducing the spectra with more concentrated samples. Spectral shapes and features in the Soret region were similarly verified using more dilute samples.

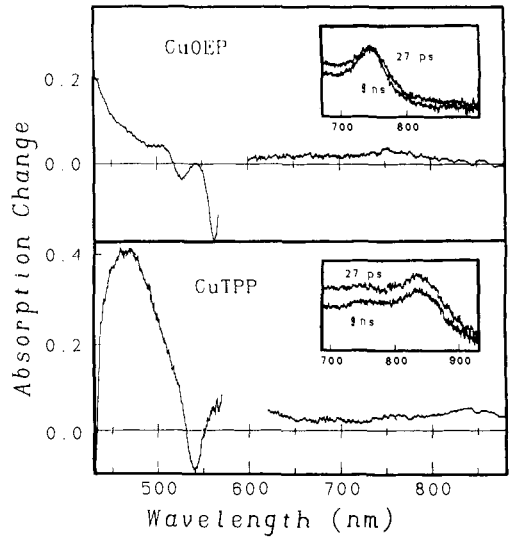

Figure 4. Absorption difference spectra measured 20 ps after excitation of $Cu^{II}OEP$ (top panel) and $Cu^{II}TPP$ (lower panel) with a 582-nm 350-fs flash. The insets show near-infrared region spectra measured 27 ps and 9 ns after excitation with a 30-ps 532-nm flash.

Results

Visible/near-infrared absorption difference spectra have been determined for the $^1(\pi,\pi^*)$ and $^3(\pi,\pi^*)$ excited states of the Sn(IV), Zn(II), Mg(II), and free-base (metal-free) complexes of octaethylporphyrin (OEP) and tetraphenylporphyrin (TPP). Spectra for six of these complexes are shown in Figures 1–3, and important features in the (π,π^*) spectra of all of these compounds are summarized in Table I. The $^1(\pi,\pi^*)$ spectra were measured shortly after the excitation flash, while the $^3(\pi,\pi^*)$ spectra were measured at a much longer delay time, after the singlet had decayed.[8] Along the series of complexes the $^1(\pi,\pi^*)$ lifetime increases as follows: ~700 ps for the Sn(IV) compounds, ~2.5 ns for Zn(II), ~9 ns for Mg(II), and ~12 ns for the free-base complexes. These lifetimes are known from either direct lifetime measurements via fluorescence or transient absorption and/or can be calculated from the fluorescence yields and natural singlet lifetimes of ~60 ns for the metal complexes and ~120 ns for the free-base compounds.[5a,j,l,9] (We verified that these lifetimes are approximately as expected.) Because the maximum pump–probe delay on the femtosecond apparatus is about 4 ns, the triplet–triplet spectra of the Mg(II) and free-base complexes were recorded in solutions containing 20% MeI, which increases the rate of singlet–triplet intersystem crossing and appreciably shortens the $^1(\pi,\pi^*)$ lifetime.[10] The insets to Figures 1 and 2 show an expanded view of the near-infrared regions of both the singlet and

(8) The evolution of spectral features on a time scale < 10 ps may contain a contribution from vibrational relaxation processes, which should be given careful consideration when attempting to assign ultrafast spectral behavior to electronic events.[12d,22] This is especially true when the energy of the photon far exceeds the energy of the excited state. With extensive averaging we were able to resolve minor (<10% of the overall signal) distortions of the Q(0,1) stimulated emission that relaxed in about 10 ps. This behavior, which appears to be enhanced at higher excitation intensities, probably arises from the small fraction of the excited molecules that may absorb a second photon[7c] and that slowly (~10 ps) dissipate their large excess energy into the solvent.

(9) (a) Gouterman, M. In *The Porphyrins*; Dolphin, D., Ed.; Academic Press: New York, 1978; Vol. 3, p 1. (b) Beddard, G. S.; Fleming, G. R.; Porter, G.; Robbins, R. *Philos. Trans. R. Soc. London, A* **1980**, *298*, 321.

(10) For example, the lifetime of the $^1(\pi,\pi^*)$ state of H_2OEP in toluene/20% MeI is reduced to 870 ps from ~12 ns in the absence of the heavy-atom solvent. We verified that the $^1(\pi,\pi^*)$ spectra were the same with and without MeI, giving us confidence that the $^3(\pi,\pi^*)$ spectra are not distorted by the addition of MeI. (We find in general that the (π,π^*) excited-state spectra are not particularly solvent dependent.) We also measured the red region of triplet–triplet absorption spectra of the Zn(II) and Mg(II) complexes at a 12-ns delay on the picosecond spectrometer, which yielded the same features as those obtained on the femtosecond apparatus. Our $^3(\pi,\pi^*)$ spectra for the Zn(II), Mg(II), and free-base TPP complexes are in excellent agreement in the regions of overlap with the point-by-point spectra obtained on the microsecond and slower time scales.[4,5b] The spectra for $Sn^{IV}TPPCl_2$ in the region between 400 and 550 nm agree with those obtained previously in this region.[5j]

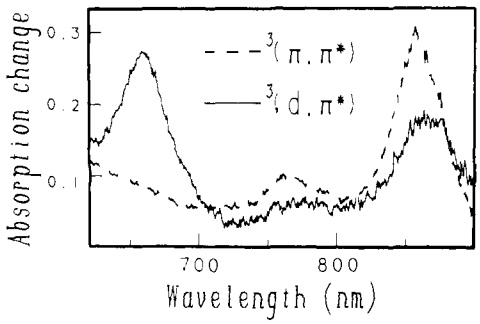

Figure 5. Absorption difference spectra for the $^3(\pi,\pi^*)$ excited state of $Ru^{II}TPP(CO)(pip)$ (---) and the (d,π^*) excited state of $Ru^{II}TPP(pip)_2$ (—) measured in piperidine 50 ps after a 30-ps 532-nm flash.

triplet absorption spectra, usually obtained with samples more concentrated than those used for the main part of each figure.

For some metalloporphyrins, intersystem crossing into the triplet manifold was found to occur so rapidly (<350 fs) that we were not able to resolve the process. For example, we found this to be the case for $Cu^{II}TPP$ and $Ru^{II}TPP(CO)(pip)$ (pip = piperidine). Figure 4 shows the visible/near-infrared absorption difference spectra for $Cu^{II}OEP$ and $Cu^{II}TPP$. The unpaired metal electron in these d^9 complexes splits $^3(\pi,\pi^*)$ into a tripdoublet $^2T(\pi,\pi^*)$ and a quartet $^4T(\pi,\pi^*)$,[9a] which are responsible for the spectra in Figure 4.[11] The dashed spectrum in Figure 5 shows the long-wavelength transient absorption of the $^3(\pi,\pi^*)$ excited state of $Ru^{II}TPP(CO)(pip)$. This near-infrared spectrum is very representative of those obtained for a variety of Ru(II) carbonyl porphyrins.[6]

The general characteristics of the $^1(\pi,\pi^*)$ and $^3(\pi,\pi^*)$ spectra can be summarized as follows:

(1) The $^1(\pi,\pi^*)$ and $^3(\pi,\pi^*)$ states both show strong absorption between 420 and 490 nm, i.e., between the Soret-band and Q-(1,0)-band bleachings. There appears to be more that one underlying component to the excited-state absorption in this region for both excited states.

(2) The spectra of both the $^1(\pi,\pi^*)$ and $^3(\pi,\pi^*)$ excited states contain a broad absorption extending from 500 nm through the near-infrared.

(3) The $^1(\pi,\pi^*)$ spectra display a characteristic Q(0,1) stimulated emission band, which appears as a negatively going feature embedded in the background absorption to the red of the Q-band bleachings. (The stimulated emission augments the intensity of the probe pulse and therefore appears as an absorption decrease in the difference spectrum.) The position of Q(0,1) stimulated emission coincides with the position of Q(0,1) spontaneous emission (fluorescence). Hence, Q(0,1) stimulated emission occurs in the vicinity of 650 nm for the metalloporphyrins and near 700 nm for the free-base complexes. The absorption decrease in the Q(0,0) region of the singlet spectrum contains contributions from *both* Q(0,0) stimulated emission and bleaching of the Q(0,0) ground-state absorption band.

(4) The $^3(\pi,\pi^*)$ spectrum is marked by a distinct near-infrared absorption peak, which is not seen in the $^1(\pi,\pi^*)$ spectrum. This feature, which always appears at the long-wavelength edge of the broad background absorption, is normally located between 820 and 850 nm for the TPP complexes investigated and at a shorter wavelength and more variable position (710–800 nm) for the corresponding set of OEP complexes. There is an indication in many of the triplet spectra that there is a second, smaller feature located 1400–1500 cm^{-1} to the blue of this main near-infrared absorption band. This double-banded nature of the near-infrared region of the $^3(\pi,\pi^*)$ spectra is seen most clearly in $Zn^{II}TPP$ (Figure 2, lower inset) and in the Ru(II) complexes (dashed spectrum in Figure 5).

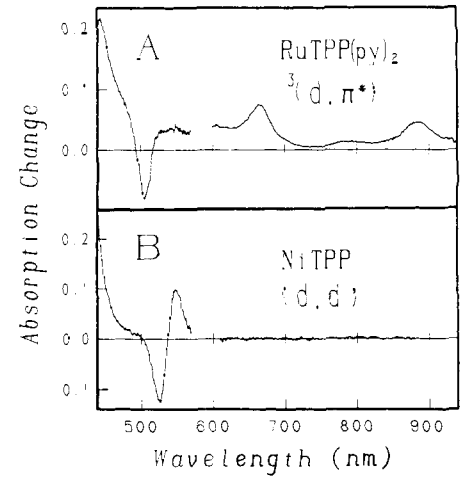

Figure 6. (A) Absorption difference spectrum of the (d,π^*) excited state of $Ru^{II}TPP(py)_2$ in pyridine, measured 20 ps after a 350-fs 582-nm excitation flash. (B) Absorption difference spectrum of the (d,d) excited state of $Ni^{II}TPP$ in toluene, measured 20 ps after a 350-fs 582-nm excitation flash.

The spectra of the $^3(d,\pi^*)$ metal-to-ring charge-transfer excited states of $Ru^{II}TPP(pip)_2$ and $Ru^{II}TPP(py)_2$ are shown in Figure 5 (solid) and Figure 6A, respectively. The $^3(d,\pi^*)$ state has been assigned previously as the lowest excited state of these complexes, and it has been shown that this state is present shortly after picosecond excitation.[6b] The $^3(d,\pi^*)$ states of $Ru^{II}TPP(pip)_2$ and $Ru^{II}TPP(py)_2$ have lifetimes of 2 and 12 ns, respectively, which are about 1000 times shorter than the lifetimes of 4 and 30 μs for $^3(\pi,\pi^*)$ in the corresponding $Ru^{II}TPP(CO)(L)$ complexes.[6b,d] The $^3(d,\pi^*)$ state, unlike the $^3(\pi,\pi^*)$ state, shows a prominent absorption band at 660 nm in addition to two smaller features in the vicinity of the two bands in the $^3(\pi,\pi^*)$ spectrum (compare spectra in Figure 5).[6c] Similar three-banded near-infrared spectra have been measured for the $^3(d,\pi^*)$ states of a variety of $Ru^{II}OEP(L)_2$ and $Ru^{II}TPP(L)_2$ complexes, where L is a σ-donor ligand.[6] We show here for $Ru^{II}TPP(py)$ that the $^3(d,\pi^*)$ spectrum also contains strong absorption in the Soret region, with a maximum near 450 nm (Figure 6A).

Finally, we report the visible/near-infrared absorption difference spectrum of a metalloporphyrin (d,d) excited state. Figure 6B shows the spectrum of the low-lying (d_{z^2}, $d_{x^2-y^2}$) excited state of $Ni^{II}TPP$. This ligand-field excited state decays with a time constant of ~250 ps in noncoordinating solvents.[7a,12] The visible spectrum is characterized by derivative-like absorption changes. Transient absorptions appear immediately to the red of the bleachings of the ground-state Soret and Q bands. Similar spectral changes have been found for a variety of four-coordinate Ni(II) porphyrins.[7a,12] Unlike the (π,π^*) and (d,π^*) excited state spectra, the (d,d) state spectrum is void of absorption changes to the red of 600 nm. We have also found this to be the case for the (d,d) state spectrum of Ni(II) protoporphyrin IX dimethyl ester.[12d]

The excited-state difference spectra can be put on a more quantitative footing by converting the absorption changes into differential extinction coefficients, i.e., $\Delta\epsilon = \epsilon$(excited state) – ϵ(ground state). Of course, in spectral regions where the ground state does not absorb (e.g., to the red of the Q bands and, often, between the Soret and Q bands), the differential extinction coefficient is simply the extinction coefficient of the excited-state

(11) (a) It appears that the tripdoublet forms from the initially excited singdoublet in less that a picosecond, with subsequent establishment of the $^2T \leftrightarrow {}^4T$ equilibrium in <500 ps.[5i,11b,c] The small decay between 27 ps and 9 ns in the insets in Figure 4 reflects in part establishment of this equilibrium and in part the beginning of the decay[11d,e] of the $^2T/{}^4T$ manifold. (b) Kobayashi, T.; Huppert, D.; Straub, K. D.; Rentzepis, P. M. *J. Chem. Phys.* **1979**, *70*, 1720–1726. (c) Chirvonyi, V. S.; Dzhagarov, B. N.; Gurinovich, G. P. *Bull. Acad. Sci. USSR Phys. Ser.* **1984**, *48*, 55. (d) Yan, X.; Holten, D. *J. Phys. Chem.* **1988**, *92*, 5982–5986; (e) Asano, M.; Kaizu, Y.; Kobayashi, H. *J. Chem. Phys.* **1988**, *89*, 6567–6576.

(12) (a) Kim, D.-H.; Holten, D. *Chem. Phys. Lett.* **1983**, *98*, 584–589; (b) Chirvonyi, V. S.; Dzhagarov, B. M.; Timinskii, B. M.; Gurinovich, G. P. *Chem. Phys. Lett.* **1980**, *70*, 79–83. (c) Kobayashi, T.; Straub, K. D.; Rentzepis, P. M. *Photochem. Photobiol.* **1979**, *29*, 925–931; (d) Rodriguez, J.; Holten, D. *J. Chem. Phys.*, in press. (e) In ref 12b and 12d the spectra of the (d,d) excited state are carried through the Soret band, showing the derivative-like absorption changes in this region.

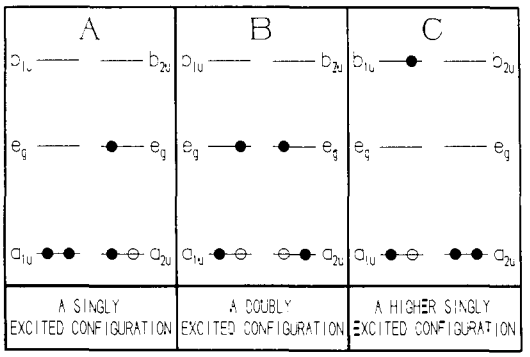

Figure 7. Schematic molecular orbital diagrams depicting several electronic configurations that may contribute significantly to the lowest (π,π^*) excited states of porphyrins. The $a_{1u}(\pi)$ and $a_{2u}(\pi)$ orbitals are the top HOMOs and the $e_g(\pi^*)$ are the lowest LUMOs (D_{4h} symmetry notation), and form the basis for the four-orbital model for porphyrin spectroscopy.[9a,13,19] Note that the relative energies of $a_{1u}(\pi)$ and $a_{2u}(\pi)$ and also the $b_{1u}(\pi^*)$ and $b_{2u}(\pi^*)$ orbitals vary among the complexes and normally would not be expected to have the same energy.

absorption. The method we adopted for assessing the extinction coefficients of the features in the excited-state spectra is to reference the magnitude of the absorption change at a particular wavelength to the size of the bleaching of the Q(1,0) ground-state absorption band (referenced to the positive background absorption).

The results of these estimates are given in Table I for the $^1(\pi,\pi^*)$ and $^3(\pi,\pi^*)$ states. The maximum transient absorption in the 420–490-nm region for both the $^1(\pi,\pi^*)$ and the $^3(\pi,\pi^*)$ excited states has an average amplitude about 3 times larger than the magnitude of the Q(1,0) bleaching, corresponding to an excited-state extinction coefficient of $\sim$50 mM^{-1} cm^{-1} (Table I). At longer wavelengths, the amplitude of the near-infrared maximum in the $^3(\pi,\pi^*)$ spectrum is on the average 3 times smaller than the size of the Q(1,0) bleaching and thus has an extinction coefficient of about 6 mM^{-1} cm^{-1}. Our $^3(\pi,\pi^*)$ extinction coefficients for the Zn(II), Mg(II), and free-base TPP complexes are in excellent agreement with the values obtained from slower time-scale measurements.[4,5b,l] The relative Q(1,0)-band bleachings (referenced to the positive background absorption) in the $^1(\pi,\pi^*)$ and $^3(\pi,\pi^*)$ spectra indicate that the triplet quantum yields are high (80–95%) for all of the complexes. In situations where 20% MeI was added, the triplet yields are essentially unity.

The Soret-region absorption of the $^3(d,\pi^*)$ state of $Ru^{II}TPP(py)_2$ and the (d,d) state of the four-coordinate Ni^{II} porphyrins has approximately the same strength as that found for the $^1(\pi,\pi^*)$ and $^3(\pi,\pi^*)$ states. The near-infrared absorption maximum in the $^3(d,\pi^*)$ states of the bisligated Ru(II) porphyrins has about the same extinction coefficient as found for the long-wavelength band in the $^3(\pi,\pi^*)$ spectra. The additional band in the 600–700-nm region of the $^3(d,\pi^*)$ spectra has an average extinction coefficient of about 12 mM^{-1} cm^{-1}. As noted above, the (d,d) state spectra measured to date have null spectra in the near-infrared.

Discussion

A large body of experimental and theoretical work has shown that the electronic spectra of metalloporphyrins are well described by transitions between states derived from configurations of the type shown in Figure 7. For example, the ground-state Soret and Q bands arise predominantly from two nearly degenerate excited configurations $[a_{1u}(\pi),e_g(\pi^*)]$ and $[a_{2u}(\pi),e_g(\pi^*)]$, which are strongly coupled by configuration interaction.[13] (The latter singly excited configuration is shown in Figure 7A). However, the absorption of the (π,π^*) excited states themselves involve transitions to states derived from other, more highly excited configurations of the type shown in Figure 7B,C.

This work has shown that both the $^1(\pi,\pi^*)$ and the $^3(\pi,\pi^*)$ excited states of porphyrins absorb very strongly in the 400–500-nm region. Following Gouterman's early semiempirical calculations[14] on the $Zn^{II}TPP$ triplet spectrum[4] and in view of our results, it seems reasonable to suppose that in general the (π,π^*) excited-state absorption in this region may arise from transitions from $^1(\pi,\pi^*)$ or $^3(\pi,\pi^*)$ to excited states derived mainly from doubly excited four-orbital configurations (e.g., Figure 7B). Within the context of the four-orbital model, this means that the first HOMO → LUMO electron promotion, $[a_{1u}(\pi),a_{2u}(\pi)] \rightarrow [e_g(\pi^*),e_g(\pi^*)]$, does not perturb the electronic system so much as to prevent the states derived from the second promotion involving these same orbitals from also absorbing strongly in the blue region of the spectrum. Support for this basic point of view can be gleaned from the spectra of the ring anions and cations. The removal of an electron from $a_{1u}(\pi)$ or $a_{2u}(\pi)$ to give the cation or addition of an electron to one of the $e_g(\pi^*)$ orbitals to give the anion yields a species that still absorbs strongly in the blue.[15-17] Calculations[15,16a,17a] on the porphyrin ions suggest that the strong blue-region absorption observed for these species contains a major contribution from four-orbital transitions similar to those just discussed for the (π,π^*) excited states.

Along these same lines, we expect strong blue-region absorption for (d,π^*) and (π,d) excited states, since the spectra of these CT should *roughly* resemble the spectra of the ring anions or cations, respectively. It is, therefore, not surprising that we have found (Figure 6A) a strong transient absorption near 450 nm for the metal → ring $^3(d,\pi^*)$ charge-transfer excited state of $Ru^{II}(TPP)(py)_2$.

The spectrum of the lowest (d,d) excited state of four-coordinate Ni(II) porphyrins also shows strong transient absorption immediately to the red of the Soret-band (and Q-band) bleaching (Figure 6B and ref 7a and 12). Similar derivative-like absorption difference spectra have been obtained for the (d,d) excited state of $Co^{III}OEP(CN)$.[18a,b] This seems quite reasonable, based on knowledge[9a,13,19] of how the metal affects the ground-state absorption spectra of metalloporphyrins. Formation of a (d,d) excited state leaves the porphyrin ring essentially in its ground-state electronic configuration, so the absorption spectrum of a ligand-field excited state should be basically the same as the ground-state spectrum, but having slightly shifted absorption bands as a result of the metal perturbation.[18c]

Similarly, it is well-known for many metalloporphyrins that changing the coordination state of the metal often results in a shifted Soret band. Thus, transient states arising from photoinduced ligand binding/release also are expected to have strong transient absorption near the Soret-band bleachings. Furthermore, spectral broadening mechanisms such as photoinduced molecular heating and conformational changes accompanying a change in electronic state also may contribute to the Soret-region transient absorption on a picosecond time scale.[2,12d,22a]

In view of our results and this discussion, we therefore emphasize that *a large absorption increase in the spectral region between 400 and 500 nm should be viewed very cautiously as being indicative of a particular transient state.* This is particularly

(13) Gouterman, M. *J. Chem. Phys.* **1959**, *30*, 1139–1161.

(14) Gouterman, M. *J. Chem. Phys.* **1960**, *33*, 1523–1529.

(15) Felton, R. H. In *The Porphyrins*; Dolphin, D., Ed.; Academic Press: New York, 1978; Vol. 5, p 53.

(16) (a) Maslov, V. G. *Opt. Spectrosc.* **1976**, *40*, 275–279. (b) Sidirov, A. N. *Biophysica* **1967**, *5*, 788–793; (c) *Ibid.* **1973**, *1*, 144–147.

(17) (a) Edwards, D. W.; Zerner, M. C. *Can. J. Chem.* **1985**, *63*, 1763–1772. (b) Furhop, J.-H.; Mauzerall, D. *J. Am. Chem. Soc.* **1969**, *91*, 4174–4181. Furhop, J.-H.; Kadish, K. M.; Davis, D. G. *J. Am. Chem. Soc.* **1973**, *95*, 5140–5147. (c) Fajer, J.; Borg, D. C.; Forman, A., Dolphin, D.; Felton, R. H. *J. Am. Chem. Soc.* **1970**, *92*, 3451–3459. (d) Dolphin, D.; Felton, R. H. *Acc. Chem. Res.* **1974**, *7*, 26–32.

(18) (a) Tait, C. D.; Holten, D.; Gouterman, M. *Chem. Phys. Lett.* **1983**, *100*, 268–272. (b) Tait, C. D., Holten, D.; Gouterman, M. *J. Am. Chem. Soc.* **1984**, *206*, 6653–6659. (c) Both the $(d_{z^2}, d_{x^2-y^2})$ excited state of the d^8 four-coordinate Ni(II) porphyrins and the (d_π, d_{z^2}) excited state of the d^6 complex $Co^{III}OEP(CN)$ show red-shifted compared to the ground-state Soret and Q bands. Other types of metalloporphyrin (d,d) excited states may show blue-shifted bands, depending on the metal orbitals involved.

(19) (a) Zerner, M.; Gouterman, M. *Theor. Chim. Acta* **1966**, *4*, 44–63. (b) Spellane, P. J.; Gouterman, M.; Antipas, A.; Kim, S.; Liu, Y. C. *Inorg. Chem.* **1980**, *19*, 386–391. (c) Shelnutt, J. A.; Oritz, V. *J. Phys. Chem.* **1985**, *89*, 4733–4739.

relevant to the analysis of the femtosecond/picosecond timescale absorption changes observed in the blue region of the spectrum following excitation of heme proteins (see ref 2 and 20–22 and citations therein). All of the types of metalloporphyrin excited states examined in this work as well as deligated/ligated transient states may be formed in heme complexes,[21] and, again, most if not all absorb strongly immediately to the red of the Soret-band bleaching.

In contrast, useful differences appear to exist between the spectra of $^1(\pi,\pi^*)$, $^3(\pi,\pi^*)$, $^3(d,\pi^*)$, and (d,d) excited states in the 600–900-nm region. One example is illustrated in the Ru(II) porphyrin data shown in Figure 5. In these complexes the nature of the lowest excited state, a $^3(\pi,\pi^*)$ state of the ring vs a $^3(d,\pi^*)$ charge-transfer state, is controlled by the σ-donating and π-accepting character of the two axial ligands.[6,23a] Similar ligand control of the lowest excited state has been observed for Os(II) porphyrins.[5e,f,23] In spite of similarities in the 700–900-nm region of the $^3(\pi,\pi^*)$ and the $^3(d,\pi^*)$ states, it is clear that the $^3(d,\pi^*)$ state has an additional relatively intense 650–700-nm band not seen in the $^3(\pi,\pi^*)$ spectra. This prominant band in the $^3(d,\pi^*)$ excited state spectrum (Figures 5 and 6A) also is present in the spectra of the ring π-anions, as are the weaker bands to longer wavelengths and the strong absorption in the vicinity of 450-nm.[15,16]

The similarities we observe in the 700–900-nm region in the spectra of the $^3(d,\pi^*)$ and $^3(\pi,\pi^*)$ states are not suprising, considering the electronic configurations of the two excited states. The $^3(\pi,\pi^*)$ state is expected to be composed mainly of the two excited four-orbital configurations $[a_{1u}(\pi),e_g(\pi^*)]$ or $[a_{2u}(\pi),e_g(\pi^*)]$ (e.g., Figure 7A),[14,24] while the (d,π^*) state is given in the most naive picture by an excited configuration $[d,e_g(\pi^*)]$. The formation of both excited states thus involves the placement of one electron in one of the $e_g(\pi^*)$ LUMOS of the ring, but in the charge-transfer state the ring HOMOs $a_{1u}(\pi)$ and $a_{2u}(\pi)$ remain filled. Thus, the absorption spectra of both excited states may share near-infrared bands whose origins can be traced in part to the electron promotions $e_g(\pi^*) \rightarrow [b_{1u}(\pi^*)$ or $b_{2u}(\pi^*)]$. Such promotions were, in fact, originally invoked by Gouterman[14] to explain the presence of the peaks to the red of 700 nm in the $Zn^{II}TPP$ $^3(\pi,\pi^*)$ spectrum;[4] such near-infrared features have now been seen for a variety of complexes (see Figures 1–4 and ref 5b,d,e,k, 6, and 25). Ab initio calculations by Petke et al. on Mg(II) porphine place a transition of this type near 800 nm but with an oscillator strength much smaller than we observe.[24a] Similarly, it has been suggested for the ring π-anion radicals (and one might expect roughly a similar situation for (d,π^*) CT states) that the long-wavelength near-infrared peak also arises largely from a transition to a state derived from the electron promotion $e_g(\pi^*) \rightarrow b_{1u}(\pi^*)$.[15,16a]

The positions of the long-wavelength feature in the near-infrared $^3(\pi,\pi^*)$ spectra appear to have a stronger metal sensitivity for OEP complexes than for TPP, as can be seen in the last two columns of Table I. The distinctive difference between the two macrocycles suggests that the terminal "b" orbital in the proposed $e_g(\pi^*) \rightarrow [b_{1u}(\pi^*)$ or $b_{2u}(\pi^*)]$ transition in the OEP complexes places considerable charge density at the nitrogens, which are more susceptible to perturbation by the metal. This would be the case if the terminal orbital were b_{2u}. On the other hand, the results for TPP are consistent with a transition to an orbital such as b_{1u} which has nodes at the central nitrogens.

Finally, we note another trend in the near-infrared features in the $^3(\pi,\pi^*)$ spectra. The observed energy spacing between the near-infrared features (when more than one feature is clearly resolved) is 1400–1500 cm^{-1}. For example, the triplets of a variety of $Ru^{II}TPP(CO)(ligand)$ complexes have two near-infrared bands that typically occur near 850 and 760 nm, whereas they can be found near 800 and 720 nm for the OEP complexes (Figure 5 and ref 6).[26] This 1400–1500-cm^{-1} spacing is not much different from the vibrational spacing normally found in the emission from the $^1(\pi,\pi^*)$ and $^3(\pi,\pi^*)$ states.[9a] This spacing in the $^3(\pi,\pi^*)$ spectrum does not appear to be particularly sensitive to the peripheral substituents on the macrocycle or to the electronic configuration of the metal. We therefore suggest that the higher energy near-infrared band in $^3(\pi,\pi^*)$ spectra may represent a vibrational overtone of the stronger low-energy band assigned above.

Perhaps the most prominent, and very useful, characteristic of the $^1(\pi,\pi)$ difference spectrum is the Q(0,1) stimulated emission, which appears as a distinct negatively going feature to the red of the Q-band bleachings. This feature arises from the gain that the weak probe pulse experiences as it stimulates the excited molecule to emit. The stimulated emission, just as the more familiar ground-state "stimulated" absorption, is not an artifact of high excitation intensities, but its amplitude is, of course, dependent (linearly) on the Q(0,1) extinction coefficient and the number of molecules placed in the $^1(\pi,\pi^*)$ excited state by the excitation flash. The Q(0,1) stimulated emission, which is typically shifted from Q(0,0) by about 1500 cm^{-1},[27] thus provides an unmistakable and convenient marker of the $^1(\pi,\pi^*)$ state, because its strength and spectral location can be easily estimated from the ground-state absorption spectrum or determined more directly from the spontaneous fluorescence spectrum. Further, the decay of the simultated emission serves as an additional measure of the lifetime of the excited singlet state and has proven to be a useful probe of the excited primary electron donor in photosynthetic reaction centers[1] and of electron and energy transfer in porphyrin dimers.[25]

In contrast to the $^3(\pi,\pi^*)$ state spectra, which exhibit distinct absorption peaks in the 600–900-nm region, we find no evidence for a clear band in this region of $^1(\pi,\pi^*)$ spectra. It should be noted that the broad featureless absorption that is observed in the $^1(\pi,\pi^*)$ spectra is, however, moderately intense, with an average extinction coefficient of 3–6 mM^{-1} cm^{-1} in the 600–800-nm region.[28] We searched in the red to ~1100 nm for a peak in the $^1(\pi,\pi^*)$ spectrum of $Zn^{II}TPP$ (data not shown) but found only a continuation of the monotonically decreasing featureless transient absorption.

Finally, our comments above regarding the fact that the (d,d) excited-state spectra are similar to the ground-state spectra but slightly shifted implies that these ligand-field states should have

(20) (a) Petrich, J. W.; Poyart, C.; Martin, J. L. *Biochemistry* **1988**, *27*, 4049–4060. (b) Jongeward, K. A.; Magde, D.; Taube, D. J.; Marsters, J. C.; Traylor, T. G.; Sharma, V. S. *J. Am. Chem. Soc.* **1988**, *110*, 380–387. James, S. M.; Dalickas, G. A.; Eaton, W. A.; Hochstrasser, R. M. *Biophys. J.* **1988**, *54*, 545–549.

(21) (a) Cornelius, P. A.; Steele, A. W.; Chernoff, D. A.; Hochstrasser, R. M. *Proc. Natl. Acad. Sci. U.S.A.* **1981**, *78*, 7256–7259. (b) Rawlings, D. C.; Gouterman, M.; Davidson, E. R.; Feller, D. *Int. J. Quantum Chem.* **1985**, *28*, 773–796.

(22) (a) Henry, E. R.; Eaton, W. A.; Hochstrasser, R. M. *Proc. Natl. Acad. Sci. U.S.A.* **1986**, *83*, 8982–8986. (b) Petrich, J. W.; Martin, J. L.; Houde, D.; Poyart, C.; Orsag, A. *Biochemistry* **1987**, *26*, 7914–7923.

(23) (a) Antipas, A.; Buchler, J. W.; Gouterman, M.; Smith, P. D. *J. Am. Chem. Soc.* **1978**, *100*, 3015–3024. (b) Antipas, A.; Buchler, J. W.; Gouterman, M.; Smith, P. D. *J. Am. Chem. Soc.* **1980**, *102*, 198–207.

(24) (a) Petke, J. D.; Maggiora, G. M.; Shipman, L. L.; Christoffersen, R. E. *J. Mol. Spectrosc.* **1978**, *71*, 64–84. (b) Gouterman, M.; Howell, D. B. *J. Phys. Chem.* **1974**, *61*, 3491–3492.

(25) (a) Mataga, N.; Yao, H.; Okada, T.; Kanda, Y.; Harriwan, A. *Chem. Phys.* **1989**, *131*, 473–480. (b) Sessler, J.; Johnson, M.; Creager, S.; Fettinger, J.; Ibers, J. A.; Rodriguez, J.; Kirmaier, C.; Holten, D. *Proc. 10th Int. Cong. Protobiol.*; Plenum: New York, in press.

(26) The ~20-nm red shift of the near-infrared peak in the Ru(II) porphyrin $^3(\pi,\pi^*)$ spectra compared to the other complexes (Table I) can be traced to the well-documented metal-to-ring π-backbonding[6,23a] which raises the energy of the ring $e_g(\pi^*)$ orbital and thus would lead to a decrease in the energy of the proposed $e_g(\pi^*) \rightarrow [b_{1u}(\pi^*)$ or $b_{2u}(\pi^*)]$ electron promotion.

(27) The disparity between the similar 1500-cm^{-1} shift in the spontaneous fluorescence spectrum and the 1250-cm^{-1} spacing observed in the ground-state spectrum has been previously attributed to vibronic coupling of the Q(1,0) and Soret transitions: Perrin, M. H.; Gouterman, M.; Perrin, C. L. *J. Chem. Phys.* **1969**, 50, 4137–4150.

(28) (a) Ab initio calculations by Petke et al.[24a] and INDO/S-CI calculations by Edwards et al.[17a] place transitions of the type we have discussed for the near-infrared region of the $^3(\pi,\pi^*)$ spectrum in the 600–900-nm region of the $^1(\pi,\pi^*)$ spectrum. Masthay et al.[28b] place a transition of symmetry b_{1g} at 1.0 eV in the $^1(\pi,\pi^*)$ spectrum. These transitions and others may blend into the broad transient absorption seen in the $^1(\pi,\pi^*)$ spectra: (b) Masthay, M. B.; Findsen, L. A.; Pierce, B. M.; Bocian, D. F.; Lindsey, J. S.; Birge, R. R. *J. Chem. Phys.* **1986**, *84*, 3901–3915.

a transparent difference spectrum in the 600–900-nm region, where the ground state usually does not absorb. We have found this to be the case in the Ni(II) porphyrins. One can generally make a similar argument concerning transient states in which an axial ligand is either bound or released in the excited state.

Thus, although the absorption changes in the red are of smaller amplitude than those in the blue, we suggest that this longer wavelength region is far more informative for the identification of metalloporphyrin transient states than is the Soret region.

Summary

In this article we have examined the optical features that characterize the $^1(\pi,\pi^*)$, $^3(\pi,\pi^*)$, $^3(d,\pi^*)$, and (d,d) excited states of a variety of metalloporphyrins. All of the excited-state spectra exhibit strong absorption between 420 and 490 nm. This observation is not surprising in view of the likely common origin of the absorption in this region—transitions to excited states derived mainly from doubly excited configurations involving the $a_{1u}(\pi)$, $a_{2u}(\pi)$, and $e_g(\pi^*)$ orbitals. One conclusion to be drawn from our work is that the observation of strong absorption between the Soret- and Q-band bleachings must be used very cautiously as being indicative of a particular transient state.

Both the $^1(\pi,\pi^*)$ and the $^3(\pi,\pi^*)$ states feature a broad absorption that spans the visible and tails toward zero in the near infrared. In addition, the spectrum of the $^3(\pi,\pi^*)$ state almost always contains an absorption peak between 700 and 850 nm that rides atop this background. A similar long-wavelength absorption band is observed in the spectrum of the $^3(d,\pi^*)$ state, which allows some insight into the electronic origins of these bands. A second, weaker near-infrared transient absorption peak in the $^3(\pi,\pi^*)$ and $^3(d,\pi^*)$ spectra normally appears about 1400–1500 cm^{-1} to shorter wavelengths, and we tentatively attribute it to a vibrational overtone of the long-wavelength transition. The spectrum of the $^3(d,\pi^*)$ state contains, in addition, a prominant band between 650 and 700 nm. The $^3(d,\pi^*)$ spectra are similar to spectra of metalloporphyrin π-anions. The observed (d,d) state spectra show a null spectrum to the red of the Q-band bleachings, as expected on the basis of straightforward electronic considerations. The $^1(\pi,\pi^*)$ excited-state spectra contain stimulated emission features that unambiguously identify this state. The Q(0,1) stimulated emission band, which appears as a negative feature that interrupts the broad transient absorption, lies $\sim$1500 cm^{-1} to the red of the Q(0,0) absorption band. On the basis of these observations, we suggest that the 600–900-nm region is better suited than the Soret region for helping to distinguish metalloporphyrin transient states. The analysis of fundamental optical properties of metalloporphyrin excited states that we have presented provides a very useful framework that will facilitate in vivo and in vitro transient absorption studies of these complexes.

Acknowledgment. This work was supported by Grant GM34685 from the National Institutes of Health.

Thermochemical Properties of Ion Complexes $Na^+(M)_n$ in the Gas Phase

B. C. Guo, B. J. Conklin, and A. W. Castleman, Jr.*

Contribution from the Department of Chemistry, The Pennsylvania State University, University Park, Pennsylvania 16802. *Received February 27, 1989*

Abstract: Enthalpy, entropy, and Gibbs free energy changes for the ion-neutral association reactions $Na^+(M)_{n-1} + M \rightleftarrows Na^+(M)_n$, where M is acetone with n = 1–4, methanol with n = 1–4, and diethyl ether with n = 1–3, were measured using high-pressure mass spectrometry. From these data and earlier values, the order of the bonding energies of Na^+M is found: $(MeOCH_2)_2$ > acetone > CH_3NH_2 > Et_2O > NH_3 > CH_3OH > H_2O > SO_2 > CO_2 > CO > HCl > N_2 > CH_4. From our ab initio calculations and those of others, the interaction of Na^+ with M is found to be due mainly to electrostatic interactions. The enthalpy changes with the number of ligands, n, shows that the stability of $Na^+(M)_n$ decreases with n, and the larger the molecular size of the ligands, the more rapidly the stability decreases. The results indicate that the rapid decrease of the stability of cluster ions formed by sodium ion with larger size ligands is attributable to strong crowding in the cluster ions.

In recent years, considerable attention has been directed to studies of the nature of clusters formed by the attachment of molecules to ions in the gas phase.[1] This has been motivated in part due to realization that studies of clusters in the gas phase provide requisite data for elucidating the nature and extent of ion–solvent interactions, which are important in solution chemistry. The results give detailed information on forces operating in individual complexes, but without interference arising from the presence of the bulk solvent. Furthermore, it is evident that research in this area is also particularly valuable in the field of interphase physics,[2] which is concerned with understanding the details of the collective effects responsible for phase transitions (nucleation phenomena), the development of surfaces, and ultimately solvation phenomenon and formation of the condensed state.

Among the various methods available to study ion clusters, high-pressure mass spectrometry (HPMS) is one of the most useful to measure their thermodynamic properties.[3-5] During past years, a number of bonding energies of metal ions with various ligands have been determined by HPMS in our laboratory.[2,5] Although the bonding energies of Na^+ with H_2O, NH_3, and other molecules have been available,[6-9] little work has been done on the interaction between Na^+ and organic molecules, especially those comprising important solvents. Systems of some interest include protic solvents

(1) Castleman, A. W., Jr.; Keesee, R. G. *Annu. Rev. Phys. Chem.* **1986**, *37*, 525.
(2) Castleman, A. W., Jr.; Keesee, R. G. *Acc. Chem. Res.* **1986**, *19*, 413.
(3) Castleman, A. W., Jr. Keesee, R. G. *Chem. Rev.* **1986**, *86*, 589.
(4) Kebarle, P. *Annu. Rev. Phys. Chem.* **1977**, *28* 455.
(5) Keesee, R. G.; Castleman, A. W., Jr. *J. Phys. Chem. Ref. Data* **1986**, *15*, 1011.
(6) Dzidic, I.; Kebarle, P. *J. Phys. Chem.* **1970**, *74*, 1466.
(7) Castleman, A. W., Jr.; Holland, P. M.; Lindsay, D. M.; Peterson, K. I. *J. Am. Chem. Soc.* **1978**, *100*, 6039.
(8) Peterson, K. L.; Märk, T. D.; Keesee, R. G.; Castleman, A. W., Jr. *J. Phys. Chem.* **1984**, *88*, 2880.
(9) Peterson, K. I. Ph.D. Thesis, University of Colorado, 1982. Castleman, A. W., Jr.; Peterson, K. I.; Upschulte, B. L.; Schelling, F. J. *Int. J. Mass Spectrom. Ion Phys.* **1983**, *47*, 203.

0002-7863/89/1511-6506$01.50/0